Effect of interfacial heat transfer on the onset of oscillatory convection in liquid bridge

Bo Xun [a,c], Kai Li [a,*], Paul Gang Chen [b], Wen-Rui Hu [a]

[a] Key Laboratory of Microgravity (National Microgravity Laboratory), Institute of Mechanics, Chinese Academy of Sciences, Beijing 100190, China
[b] Laboratoire Modélisation et Simulation Numérique en Mécanique et Génie des Procédés, UMR 6181, CNRS-Universités d'Aix-Marseille, F-13451 Marseille Cedex 20, France
[c] The Graduate School of Chinese Academy of Sciences, Beijing 100190, China

ARTICLE INFO

ABSTRACT

In present study, effect of interfacial heat transfer with ambient gas on the onset of oscillatory convection in a liquid bridge of large Prandtl number on the ground is systematically investigated by the method of linear stability analyses. With both the constant and linear ambient air temperature distributions, the numerical results show that the interfacial heat transfer modifies the free-surface temperature distribution directly and then induces a steeper temperature gradient on the middle part of the free surface, which may destabilize the convection. On the other hand, the interfacial heat transfer restrains the temperature disturbances on the free surface, which may stabilize the convection. The two coupling effects result in a complex dependence of the stability property on the Biot number. Effects of melt free-surface deformation on the critical conditions of the oscillatory convection were also investigated. Moreover, to better understand the mechanism of the instabilities, rates of kinetic energy change and "thermal" energy change of the critical disturbances were investigated

1. Introduction

Floating-zone (FZ) technique is a crucible-free process for the growth of high quality single crystal, which the melt zone is confined by the surface tension of melt free surface. However, the diameter of the grown crystal is limited under the terrestrial condition due to easy breakage of the melt zone induced by gravity. The essential reason to go to space for melt growth of single crystals lies in a promise that a substantial reduction of gravity level achieved in spacecraft may result in a quiescent melt pool, thereby allowing a diffusion-controlled growth condition to be realized. Moreover, the microgravity environment provides the possibility of growing large size crystal by the FZ technique. However, experimental facts revealed that during the FZ process in microgravity, thermocapillary flow driven by the surface tension gradient of the melt free surface, depending on such factors like temperature, solutal concentration, electric potential etc., occurs in the melt zone even when the buoyancy-driven flow is greatly reduced. The thermocapillary flow may be oscillatory when the Reynolds number exceeds certain critical value and responsible for striations in crystals grown in space [1]. Therefore, numerous experimentations and analytical studies (linear instability analyses and direct numerical simulations) have been devoted to the oscillatory thermocapillary flows in liquid bridge model (see Fig. 1) mimicking the half of FZ for the sake of simplicity during the last decades.

It is now well established that a steady axisymmetric (2D) thermocapillary flow loses its stability first to a steady asymmetric (3D flow and then to an oscillatory flow in liquid bridges of low Prandtl numbers ($Pr \leqslant 0.06$) while it loses its stability directly to an oscillatory flow (3D) in those of large Pr numbers [2]. On the other hand, the corresponding critical conditions determined through the analytical studies can not agree well with the experimental results in quantity, especially for high Pr number fluids. It is noted that most of the analytical studies on the liquid bridge were carried out with an adiabatic melt free surface assumption, i.e., there is no heat transfer across the melt free surface. In practice, interfacial heat transfer in the experimentations, especially under high temperature conditions, may play an important role in the flow dynamics (for example, see [3–8]). Kamotani et al. [3] studied the effect of interfacial heat loss in liquid bridges of high Pr fluids considering the ambient air flow. They calculated the average interfacial heat transfer rate (indicated non-dimensionally as average Biot number in their notation), and found that the critical conditions decrease with the increased heat loss when the average Biot number is less than 1.5. Melnikov and Shevtsova [7] numerically investigated the effect of interfacial heat transfer on the thermocapillary flow in a liquid bridge of Pr = 14 with aspect ratio equal 1.8 under normal gravity condition, and the ambient air temperature was assumed to equal the cold rod temperature. They found that the heat loss leads to destabilization of the flow at small

Nomenclature

A	matrix in eigenvalue problem
B	matrix in eigenvalue problem
B	Buoyant effect
D_k	mechanical dissipation
D_{th}	thermal dissipation
E_k	Kinetic energy of disturbances
E_{th}	"thermal" energy of disturbances
g	gravitational acceleration
g_0	normal gravitational acceleration, 9.806 (kg m/s^2)
h	heat transfer coefficient on free surface
h(z)	free surface local radius
i	$\sqrt{-1}$
I	interactive term in kinetic energy equation
J_i	interactive term in "thermal" energy equation decomposed in cylindrical coordinates
k	thermal conductivity coefficient
L	height of the liquid bridge
M_i	work done by thermocapillary force decomposed in cylindrical coordinates
$\vec{n}$	the outward-directed normal vector of the free surface
N_z	number of the grid points in axial direction
N_r	number of the grid points in radial direction
R	radius of the liquid bridge
$|w|_{max}$	maximal value of $|w|$ on the free surface
s	surface of the liquid bridge
S	dimensionless stress tensor, $\nabla \vec{U} + (\nabla \vec{U})^T$
T	dimensionless time
$\vec{t}_z$	the unit vector tangent to the free surface in the (r, z) plane

$\vec{t}_\varphi$	the unit vector tangent to the free surface in the (r, φ) plane
T	dimensionless temperature
T_0	mean temperature of the upper and lower ends
T_{amb}	dimensionless temperature of the ambient air
T_{cold}	dimensionless temperature on the cold rod
$\vec{U}$	dimensionless velocity vector, (u, v, w)
x	vector composed of disturbance velocity, pressure and temperature, $(u', iv', w', p', T')^T$
X	the basic steady axisymmetric state, $\{\vec{U}(r,z) = U\vec{e}_r + W\vec{e}_z, P(r,z), T(r,z)\}$
(r, θ, z)	cylindrical coordinates
V_0	the liquid volume with cylindrical shape

Greek symbols

|	
α	thermal diffusivity coefficient
β	thermal expansion coefficient
ΔT	applied temperature difference between two solid ends
γ	negative temperature gradient of surface tension
μ	dynamic viscosity coefficient
υ	kinematic viscosity coefficient
(ξ, η)	coordinates in computational domain
$|\psi|_{max}$	maximal absolute value of the stream function
ρ_0	mean density
σ_0	mean free surface tension
σ(m)	the complex growth rate of the corresponding perturbation mode
μ	dynamic viscosity coefficient
Ω	volume domain occupied by the liquid bridge
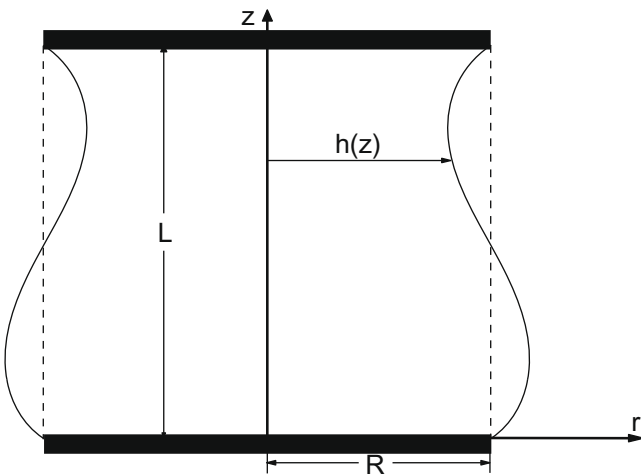
Fig. 1. Scheme diagram of a liquid bridge.

Biot numbers ($Bi \leqslant 2$) contrary to the stabilization of the flow at large Bi numbers ($Bi \leqslant 5$). Similarly, Kousaka and Kawamura [5] studied the thermocapillary flow in a liquid bridge of Pr = 28.1 with unitary aspect ratio under zero gravity condition, and a linear ambient air temperature distribution was adopted. In their case, in the range of small Bi numbers ($Bi < 1$), there is heat loss through the free surface near the cold rod and heat gain near the hot rod, and the destabilization of the thermocapillary flow by the interfacial heat transfer was also found. Recently, Wang et al. [8] studied the situation with interfacial heat gain. They found that the critical conditions are not significantly affected by the interfacial heat gain, and there is a big jump of the critical conditions when the interfacial heat transfer is changed from heat gain to heat loss [3]. How-

ever, the aforementioned results are fragmental due to the computation task of 3D direct numerical simulation, and the detailed dependency of the critical conditions on the interfacial heat transfer is still lacking. On the other hand, to the end of the manipulation of oscillatory thermocapillary flow through varying the interfacial heat exchange, extensive preliminary experimental studies should be conducted on the ground due to the scarce space experiment opportunity. Therefore, the effect of melt free-surface deformation, which is usually ignored in previous studies such as [7], should be taken into account.

In present study, linear stability analyses were conducted to systematically investigate the dependency of the critical conditions of oscillatory convection on the interfacial heat transfer under normal gravity condition with both the constant and linear ambient air temperature distributions (the studies on the corresponding cases in the microgravity environment will be reported elsewhere). Moreover, effects of melt free-surface deformation on the critical conditions of oscillatory convection were investigated.

2. Governing equations and numerical schemes

Fig. 1 shows the scheme diagram of the liquid bridge formed by 1cst oil considered in the present study. The length, velocity, pressure and time are scaled by $R, \frac{\gamma \Delta T}{\mu}, \frac{\gamma \Delta T}{R}$ and $\frac{R^2}{\upsilon}$, respectively, and the temperature measured with respect to T_0 is scaled by ΔT. The Reynolds number, Prandtl number, Grashof number, aspect ratio, Biot number and static Bond number are defined as follows, respectively,

$$Re = \frac{\gamma \Delta T R}{\mu \upsilon}, \quad Pr = \frac{\upsilon}{\alpha}, \quad Gr = \frac{g\beta \Delta T R^3}{\upsilon^2}, \quad \Gamma = \frac{L}{R}, \quad Bi = \frac{hR}{k},$$

$$Bo = \frac{\rho_0 g R^2}{\sigma_0},$$

where $\rho_0 = 818$ kg/m³, $\beta = 0.00129$/K, $\upsilon = 10^{-6}$ m²/s, $\gamma = 5.63 \times 10^{-5}$ kg/s², $k = 2.4 \times 10^{-2}$ cal/msK, $\sigma_0 = 1.69 \times 10^{-3}$ N/K. In the cylindrical coordinate (r, θ, z), the non-dimensional governing equations are as follows:

$$\nabla \cdot \vec{U} = 0 \qquad (1)$$

$$\frac{\partial \vec{U}}{\partial t} + \text{Re}\left(\vec{U} \cdot \nabla\right)\vec{U} + \nabla P = \Delta \vec{U} + \frac{Gr}{Re} T\vec{e_z} \qquad (2)$$

$$\frac{\partial T}{\partial t} + \text{Re}\left(\vec{U} \cdot \nabla\right)T = \frac{1}{Pr}\Delta T \qquad (3)$$

where $\vec{U} = (u, v, w)$ indicates the dimensionless velocity vector, P the pressure, T the temperature and t the time. The corresponding boundary conditions are as following:

$$z = 0, \quad \Gamma : \vec{U} = 0, \quad T = \mp\frac{1}{2} \qquad (4)$$

$$r = h(z) : \vec{n} \cdot \vec{U} = 0, \quad \vec{t}_z \cdot (S \cdot \vec{n}) = -\vec{t}_z \cdot \nabla T$$
$$\vec{t}_\varphi \cdot (S \cdot \vec{n}) = -\vec{t}_\varphi \cdot \nabla T, \quad \vec{n} \cdot \nabla T = -Bi(T - T_{amb}) \qquad (5)$$

where T_{amb} indicates the dimensionless ambient air temperature, $S = \nabla\vec{U} + (\nabla\vec{U})^T$ the stress tensor in non-dimensional form. The vector $\vec{n}$ is the outward-directed normal vector of the free surface, and the vectors $\vec{t}_z$ and $\vec{t}_\varphi$ denote the unit vector tangent to the melt free surface in the (r, z) plane and (r, θ) plane, respectively.

Considering the asymptotic limit of capillary number, $Ca = \frac{\gamma\Delta T}{\sigma_0} \to 0$, the melt free surface shape is symmetric to the axis of melt zone and the normal-stress balance can be approximated by the Young–Laplace equation:

$$P_s = \nabla \cdot \vec{n} + \text{Bo}z, \qquad (6)$$

where P_s is the dimensionless static pressure. Before calculating the flow and temperature fields, the free surface shape $h(z)$ is determined by Eq. (6) with the liquid bridge volume equal $\pi R^2 L$. As shown in Fig. 1, if $Bo = 0$, the free surface shape is cylindrical with $h(z) = 1$ as indicated by the dashed lines (hereafter, we use $h(z)$ to indicate the dimensionless local radius of the free surface without confusion) while $Bo \neq 0$, the free surface is curved as indicated by the solid lines. For the case with curved free surface shape, the body-fitted curvilinear coordinates are employed. The original physical domain in the (r, z) plane occupied by the liquid bridge is transformed into a rectangular computational domain in the (ξ, η) plane by the transformation $(\xi = \frac{r}{h(z)}, \eta = z)$. For the sake of brevity, the details of the transformed equations in the curvilinear coordinates (ξ, η), which is the same as the excellent work [9], are not shown here.

For the linear stability analysis, the basic steady axisymmetric state, $X = \left\{\vec{U}(r,z) = U\vec{e}_r + W\vec{e}_z, P(r,z), T(r,z)\right\}$, is first determined for a given set of parameters (Re, Pr, Bi and Γ), and then small three-dimensional disturbances are added to the basic state and linearized by neglecting high orders of disturbances [10–12]. The disturbances are assumed to be in the normal mode:

$$\begin{pmatrix} \vec{u}' \\ p' \\ T' \end{pmatrix} = \sum_{m=-\infty}^{+\infty} \begin{pmatrix} \vec{u}'^m(r,z) \\ p'^m(r,z) \\ T'^m(r,z) \end{pmatrix} \exp[\sigma(m)t + jm\phi], \qquad (7)$$

where the variables with prime denote the disturbances, m the azimuthal wave number, $\sigma(m)$ the complex growth rate of the corresponding perturbation mode, and $i = \sqrt{-1}$. The discrete form of the linearized equations can be written as a generalized eigenvalue problem:

$$g(x, X, \text{Re}, m, \text{Pr}, \Gamma, Bi) \equiv Ax = Bx, \qquad (8)$$

where $x = (u', iv', w', p', T')^T$ denotes a vector composed of disturbance velocity, pressure and temperature. A is a real-valued

non-symmetric matrix, while B is a singular real-valued diagonal matrix. The eigenvalues and related eigenfunctions of problem are solved by the Arnoldi method [13]. The critical Reynolds number Re_c is obtained when the maximal real part of $\sigma(m)$ for all m is zero.

In order to well resolve the boundary layers at both ends, a non-uniform grid with denser points near both solid ends and free surface is adopted in this study. The grid we used in the calculation is $N_r \times N_z = 81 \times 141$, where N_r and N_z indicate the number of the grid points in radial and axial direction, respectively. Moreover, to validate the present code under curved free surface situation, we reproduced some calculations in the work [9,14] using their definitions of the dimensionless numbers, and the computed results show good agreement (see Table 1).

Moreover, to better understand the mechanism of the instabilities, rates of kinetic energy (E_k) change and "thermal" energy (E_{th}) change of the critical disturbances were investigated in the following way: the disturbance equations for momentum and temperature [10–12] were multiplied by the velocity and temperature disturbances, respectively, and then integrated over the volume of liquid bridge and normalized by the mechanical dissipation (D_k) and thermal dissipation (D_{th}), respectively, thus the following equations were obtained:

$$\frac{1}{D_k}\frac{dE_k}{dt} = M_1 + M_2 + M_3 + B + I - 1, \qquad (9)$$

$$\frac{1}{D_{th}}\frac{dE_{th}}{dt} = Q + J_1 + J_2 - 1. \qquad (10)$$

where $E_k = \int_\Omega \frac{\vec{u}'^2}{2} d\Omega$, $E_{th} = \int_\Omega \frac{T'^2}{2} d\Omega$, $D_k = \int_\Omega \frac{S':S'}{2} d\Omega$, $D_{th} = \int_\Omega \frac{\nabla T' \cdot \nabla T'}{Pr} d\Omega$ are the integrations over the volume of liquid bridge (Ω), respectively, $M = -\frac{1}{D_k}\oint\oint \vec{u}' \cdot \nabla T' ds = M_1 + M_2 + M_3 = -\frac{1}{D_k}\oint\oint u'\frac{\partial T'}{\partial r} ds - \frac{1}{D_k}\oint\oint v'\frac{\partial T'}{\partial \varphi} ds - \frac{1}{D_k}\oint\oint w'\frac{\partial T'}{\partial z} ds$ the integrations over the surface of Ω denoting the work done by the thermocapillary force induced by the temperature disturbance per unit time, $B = \frac{Gr}{Re}\int_\Omega w'T' d\Omega$ the work done by the buoyant force, $I = -\frac{Re}{2}\int_\Omega \vec{u}' \cdot S \cdot \vec{u}' d\Omega$ the interactive term between the basic state stress tensor and the velocity disturbance, $Q = -\frac{Bi}{Pr}\oint\oint T'^2 ds$ the transport of "thermal" energy through the free surface, and $J = -\frac{Re}{D_{th}}\int_\Omega (\vec{u}' \cdot \nabla T)T' d\Omega = J_1 + J_2 = -\frac{Re}{D_{th}}\int_\Omega (u'\frac{\partial T}{\partial r})T' d\Omega - \frac{Re}{D_{th}}\int_\Omega (w'\frac{\partial T}{\partial z})T' d\Omega$ the interactive terms between the basic state temperature and the velocity and temperature disturbances.

Table 1
Code validation.

	Aspect ratio	Contact angle at hot rod: α_h (°)	Present code $N_r \times N_z = 51 \times 71$	Reference [9]
(a) Pr = 0.02, Re = 2000, g = 0				
$\|\psi\|_{max}$	$\Gamma = 1$	40	8.62	8.42
		140	25.04	24.67
	$\Gamma = 1.2$	40	5.76	5.61
		140	21.76	21.95
$\|w\|_{max}$ on free surface	$\Gamma = 1$	40	190.59	188.61
		140	182.05	182.95
	$\Gamma = 1.2$	40	188.39	184.46
		140	190.40	202.55

Contact angle at hot rod: α_h (°)	m	Present code $N_r \times N_z = 51 \times 71$	Reference [14]
(b) Pr = 4, Γ = 1, g = 0, Bi = 0			
30	1	1293	1350
50	1	1487	1470
	2	1449	1445
90	2	996	1010
110	2	865	840
130	2	805	800

3. Results and discussions

3.1. Constant ambient air temperature distribution ($T_{amb} = T_{cold}$)

A liquid bridge model (see Fig. 1) formed by 1cst silicone oil (Pr = 16) with $\Gamma = 1.8$ ($L = 4.5$ mm and $R = 2.5$ mm) is adopted in this subsection. With the unitary volume ratio, $V/V_0 = 1.0$, the free surface is deformed under normal gravity with the maximum of $h(z) = 1.1713$ and the minimum of $h(z) = 0.8066$. The ambient air temperature is assumed to equal the temperature of the cold rod. Therefore, the interfacial heat transfer is always heat loss from the melt to the ambient air. Fig. 2 shows the dependency of Re_c upon Bi according to the computed results listed in Table 2, and the corresponding neutral modes are all oscillatory convections with the wave number ($m = 1$). The Re_c profile in the case of under normal gravity condition ($g = g_0$, $Bo = 2.965$) exhibits a convex dependency upon the increasing heat loss. In the parameter range studied, the Re_c decreases with the increasing Bi up to $Bi \approx 1$, and this is followed by an approximately linear increase. Noted that the interfacial heat loss starts to stabilize the convection at $Bi \approx 2.5$ compared to the corresponding adiabatic case. The isotherms and streamlines of the two-dimensional axisymmetric convection at selected Re_c are shown in Fig. 3. The thermal boundary layer is developed in the neighbor region of the hot end while the isotherms in the cold corner is compressed due to the concentrated streamlines induced by the shift of vortex core to the convex part of the free surface. Note that all disturbances must satisfy the no-slip boundary conditions at the solid ends, the magnitude of the disturbances inside the boundary layers should be smaller than those outside the boundary layer, and the part of the liquid bridge with largest disturbances is the most unstable. Therefore, the stability property of the basic flow is mainly determined by the "effective" temperature gradient on the middle part of the liquid bridge [15]. From this point of view, it is useful to investigate the temperature gradient at the middle part of the free surface. It is known that the interfacial heat transfer modifies the free-surface temperature distribu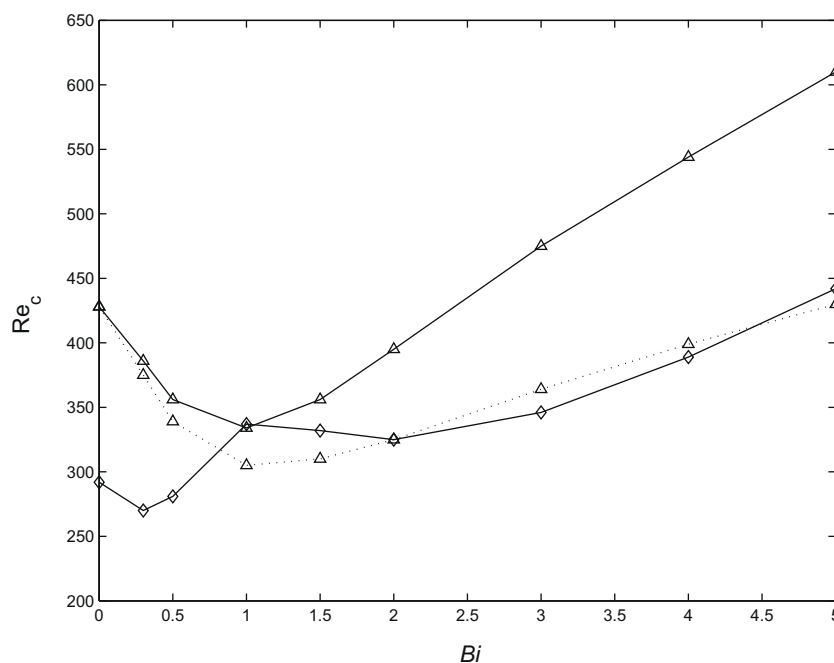tion directly and then the thermal and flow fields. In the neighbor region of the melt free surface, the increasing interfacial heat loss pulls up the isotherms near the cold end, and the temperature gradient near the cold rod is smoothed while the temperature gradient near the hot rod is enhanced. Moreover, the vortex of the flow distributes more homogeneously in the bulk region of the liquid bridge. The net effect of the above modifications is that the temperature gradient along most part of the melt free surface gets steeper with increasing Bi (see Fig. 4a). Therefore, a lower Re_c may be required to destabilize the stationary convection with increasing interfacial heat loss. On the other hand, according to the perturbation equation of the melt free-surface heat transfer:

$$\vec{n} \cdot \nabla T' = -Bi \times T' \quad \text{on} \quad r = h(z), \tag{11}$$

whenever a positive temperature disturbance appears somewhere on the melt free surface, it is accompanied by an increase of heat loss through that part of the melt free surface, and vice versa. Therefore, the interfacial heat transfer restrains the melt free-surface temperature disturbances, especially at larger Bi. To verify the remarks, Fig. 2 also shows the numerical results that Bi in the perturbation equation (11) is set to be zero. With the same basic flow, the interfacial heat transfer significantly delays the onset of the oscillatory convection, and the stabilization effect gets stronger with

Table 2
Re_c versus Bi.

Bi	$T_{amb} = -0.5$		$T_{amb} = z/\Gamma - 0.5$	
	$g = g_0$, $Bo = 0$	$g = g_0$, $Bo = 2.965$	$g = g_0$, $Bo = 0$	$g = g_0$, $Bo = 2.965$
0	292	428	292	428
0.2	–	–	275	452
0.3	270	386	–	–
0.5	281	356	257	465
1.0	337	334	240	356
1.5	332	356	234	323
2.0	325	395	234	317
3.0	346	475	247	336
4.0	389	544	270	373
5.0	442	610	293	417

Fig. 2. Critical Reynolds number versus Bi for cases of $T_{amb} = -0.5$: ($g = g_0$, $Bo = 0$) – diamond points on solid line; ($g = g_0$, $Bo = 2.965$)-triangle points on solid line and ($g = g_0$, $Bo = 2.965$) when Biot number is set to zero in the perturbation equation (11) – triangle points on the dotted line, respectively.
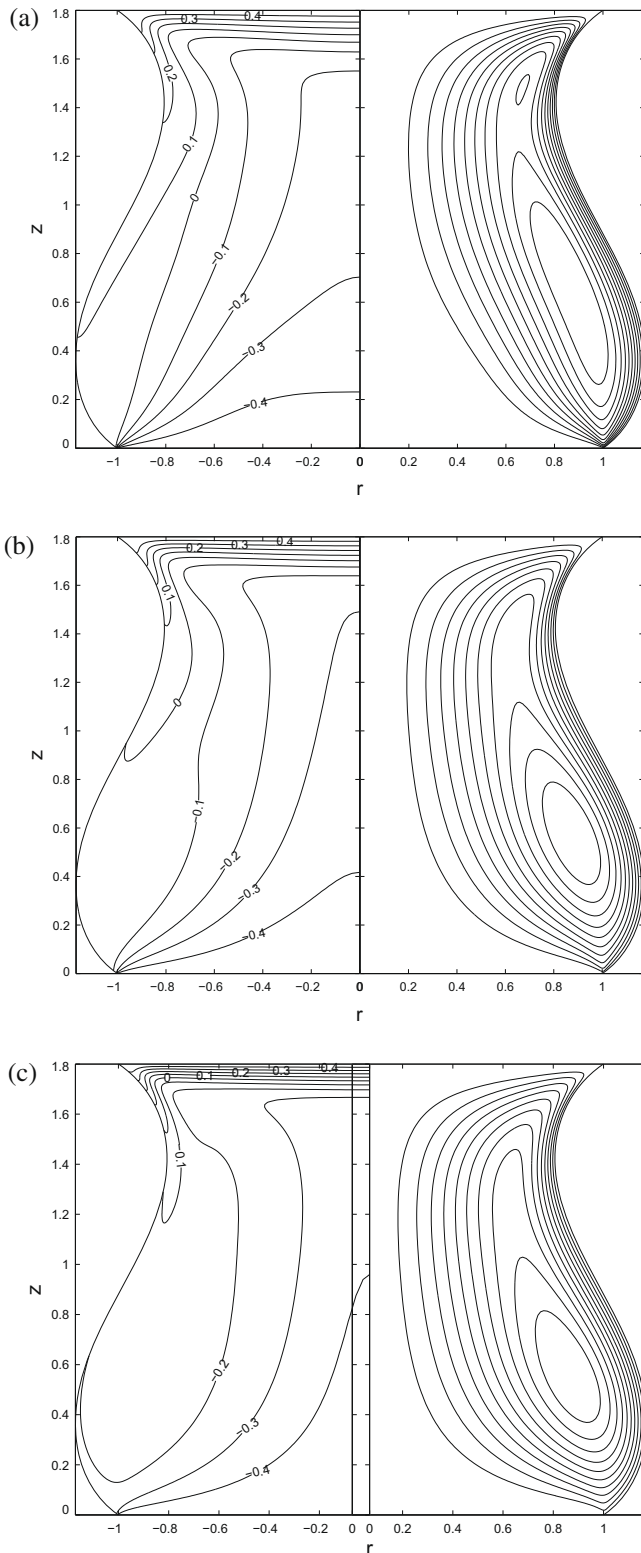
Fig. 3. Isotherms and streamlines at the corresponding Re_c for different Bi under normal gravity condition for $T_{amb} = -0.5$, $Bo = 2.965$: (a) $Bi = 0$, $Re_c = 428$; (b) $Bi = 1$, $Re_c = 356$; and (c) $Bi = 4$, $Re_c = 373$.

increasing Bi. In practice, the convex tendency of the Re_c profile shown in Fig. 2 could be due to the competition of the aforementioned two mechanisms.

For a further investigation of the physics of the instabilities, the normalized kinetic and "thermal" energy balances at selected Bi

are shown in Fig. 5a. For the "thermal" energy of the disturbance flow, the destabilizing effect (J_1) is produced by the amplification of the high radial gradient of the basic thermal field mainly occurred in the bulk through the radial flow disturbances. On the other hand, in addition to the major stabilizing effect contributed by the thermal diffusion (D_{th}), the stabilizing effects are produced by the amplification of the high axial gradient of the basic thermal field (J_2) mainly occurred near the hot end and cold corner through the axial flow disturbances [14] and the transport of "thermal" energy through the free surface (Q), the only term directly involving the effect of interfacial heat transfer. The kinetic energy is insignificant for fluids of high Pr number [14]. However, it is interesting to note that the effect of buoyant force (B) always serves the destabilization although the liquid bridge is heated from above. The rate of change of "thermal" energy with the increasing interfacial heat loss at $Re = 428$, the critical Reynolds number for the corresponding adiabatic case, is shown in Fig. 5b. It can be seen that the destabilizing effect (J_1) overwhelms the major stabilizing effect of heat diffusion (D_{th}) at small Bi, and it is overwhelmed by the heat diffusion at large Bi. The general trend of the corresponding Re_c profile is determined by the relative magnitude of (J_1) to the thermal diffusion (D_{th}). However, the details of the trend, such as the position of the local minimum, are also contributed by (J_2) at small Bi while by (Q) at large Bi.

To evaluate the effect of melt free-surface deformation on the stability of the stationary convection, an artificial case of under normal gravity condition but neglecting the melt free-surface deformation ($g = g_0$, $Bo = 0$) is studied. The numerical results show that the vortex cores in the corresponding flow fields shift to the hot corner with the crowded streamlines (not shown), which are quite different from those with deformed domain (see Fig. 3). Noted that the temperature gradient at the middle part of the melt free surface is flattened by the convection with the boundary layers formed at both the cold and hot ends where the temperature gradient increases sharply (see Fig. 4b). The corresponding Re_c profile roughly exhibits a similar tendency as the case of under normal gravity, however, with much lower quantity (see Fig. 2). It reveals the significant stabilization effect on the stationary convection through the modifications of the thermal and flow fields due to the free-surface deformation. The corresponding neutral mode keeps ($m = 1$). On the other hand, the Re_c profile exhibits a local maximum roughly at $Bi = 1$. Note that the temperature gradient distribution along the free surface exhibits the similar configuration in the middle part of the free surface except that it exhibits undulation at the lower half of the free surface in the range of small Bi (see Fig. 4b). The configuration transition of the temperature gradient distributions at $Bi = 1$ coincidently corresponds to appearance of the local maximum of the Re_c profile. The details of the relationship between the undulation of temperature gradient distribution and the sudden increasing stabilizing effect of the flow need further investigation. Similar to the case with the deformed free surface, the energy analyses for current case show that the destabilizing effect for the "thermal" energy of the disturbances flow is also produced by the radial energy transfer from the basic thermal field to the disturbance flow (J_1), and the main stabilizing effects are contributed by the thermal diffusion (D_{th}) and the axial energy transfer from the basic thermal field to the disturbance flow (J_2). Fig. 6 shows the rate of change of "thermal" energy as a function of Bi at $Re = 292$, the critical Reynolds number for the corresponding adiabatic case. It can be seen that the destabilizing effect (J_1) generally exhibits a convex trend while it keeps nearly constant in the range of Bi from 0.5 to 1.0. The stabilizing effect (J_2) also exhibits a concave trend with a local minimum at $Bi = 1.0$. The coupling of the above contra-effects and the thermal diffusion (D_{th}) results in local maximum suppressing of the instability at $Bi = 1$ in the rate of the "thermal" energy (E_{th}) change of
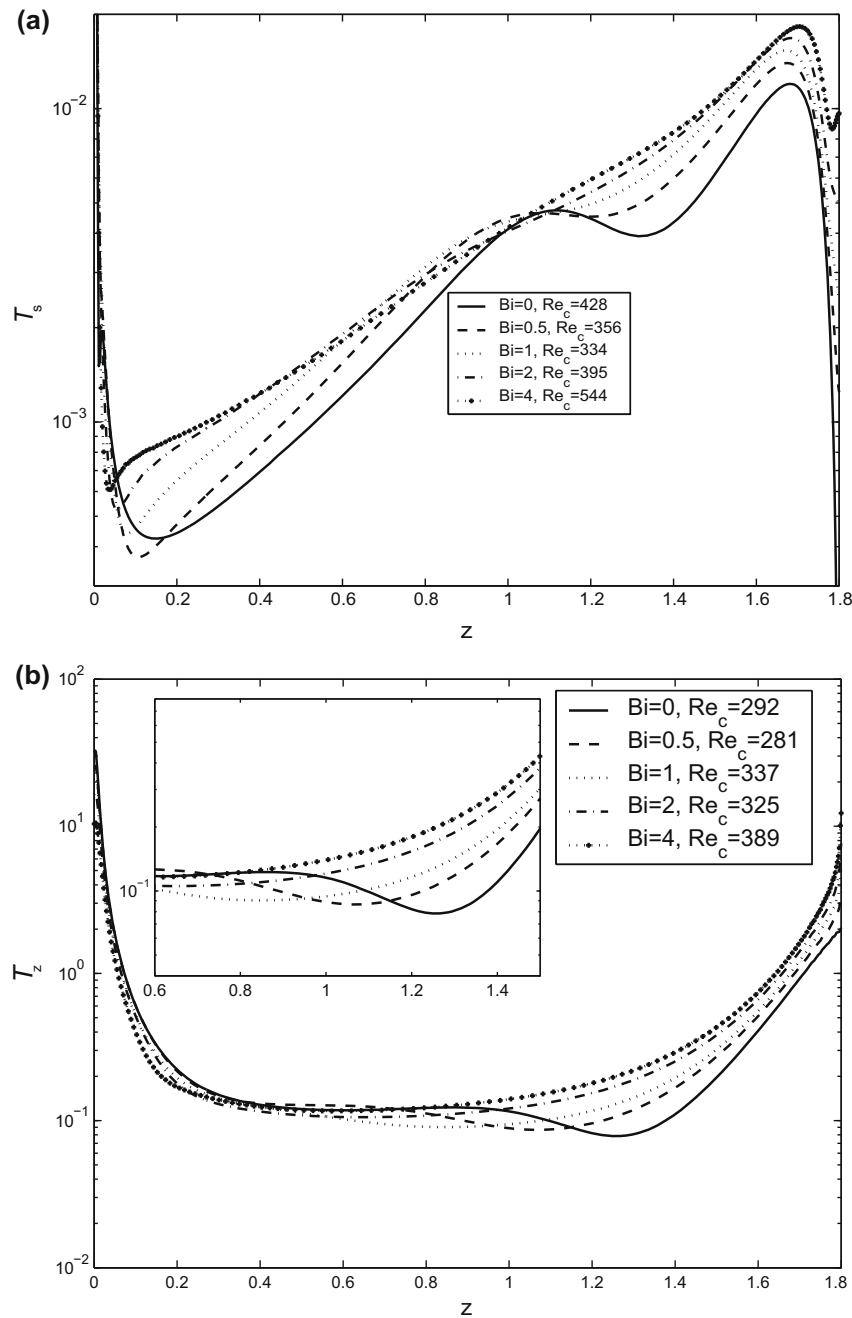
Fig. 4. Temperature gradient distribution along the melt free surface at the corresponding Re_c for $T_{amb} = -0.5$: (a) $g = g_0$, $Bo = 2.965$; (b) $g = g_0$, $Bo = 0$.

the disturbance, which corresponds to the appearance of the local maximum of the Re_c profile at $Bi = 1$.

3.2. Linear ambient air temperature distribution ($T_{amb} = z/\Gamma - 0.5$)

In this section, the same liquid bridge model as that in Section 3.1 is adopted except that the ambient air temperature is assumed to be linearly distributed along the axial direction [4,5]. Therefore, it is heat-loss to the ambient air at the lower part of the free surface while heat-gain from the ambient air at the upper part of the free surface. With the increasing interfacial heat transfer, the isotherms and streamlines of the two-dimensional axisymmetric convection (not shown) at the corresponding Re_c behave quite similarly to the case with ($T_{amb} = T_{cold}$) (see Fig. 3), so does the temperature gradient distribution on the middle part of the free surface (see Fig. 7),

which gets steeper with the increasing Bi. On the other hand, the temperature gradient at the lower part of the free surface in the present case is increased compared with Fig. 4a at the same Bi, the distributions of the "effective" temperature gradient, therefore, behave more smoothly. Fig. 8 shows the dependency of Re_c upon Bi according to the computed results also listed in Table 2. Due to the two coupling mechanisms mentioned in Section 3.1 (Fig. 8 also shows the numerical results that Bi in the perturbation equation (11) is set to be zero), the Re_c profile roughly exhibits a similar convex tendency as the corresponding case with ($T_{amb} = T_{cold}$) except the appearance of local maximum Re_c in the range of small Bi. In the parameter range studied, the wave number of the corresponding neutral mode is also ($m = 1$). The normalized kinetic and "thermal" energy balances at selected Bi are shown in Fig. 9a. In the "thermal" energy of the disturbances flow, the energy transfer
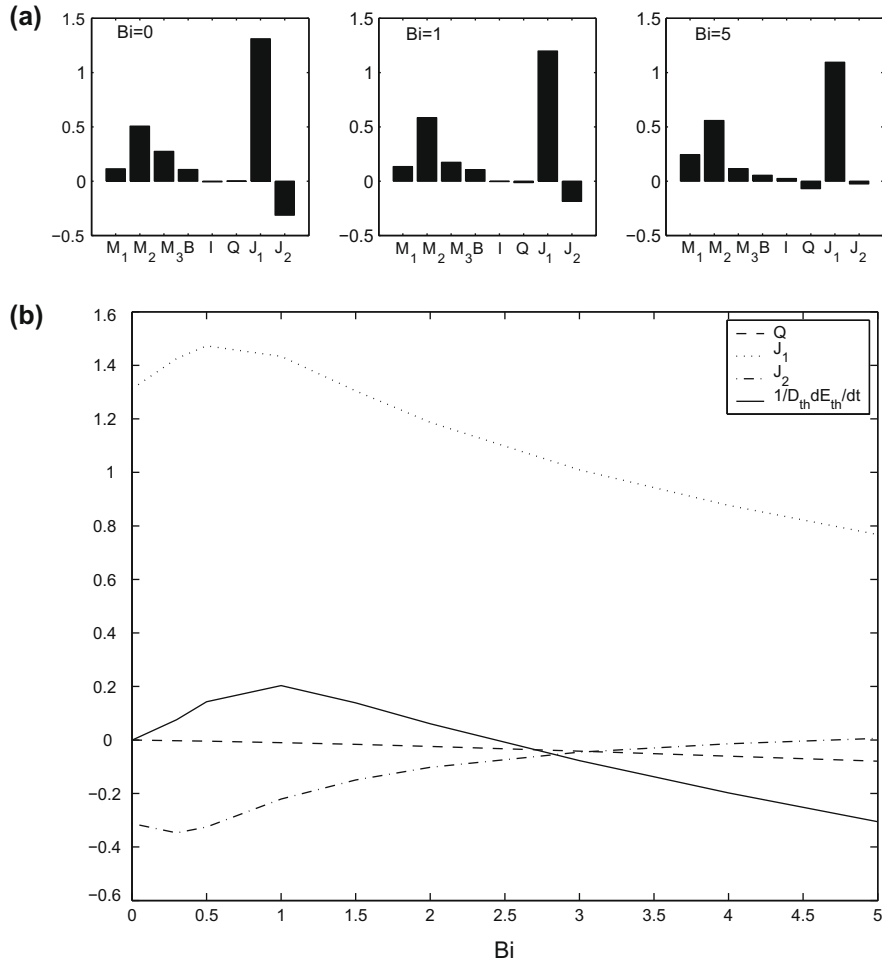
Fig. 5. Kinetic and thermal energy balance for cases of $T_{amb} = -0.5$ when $g = g_0$, $Bo = 2.965$ (a) at the corresponding Re_c and (b) at Re = 428.
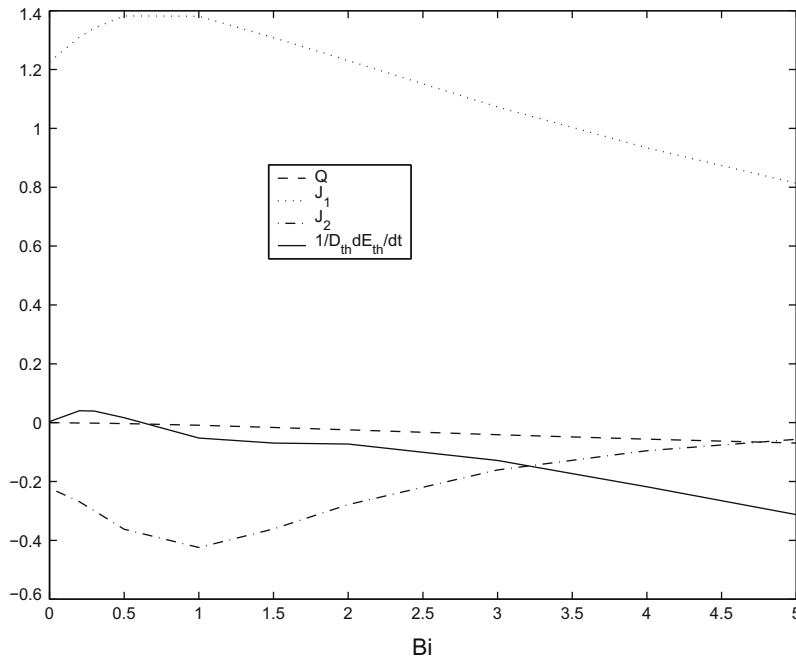

Fig. 6. Kinetic and thermal energy balance for cases of $T_{amb} = -0.5$ when $g = g_0$, $Bo = 0$ at Re = 292.
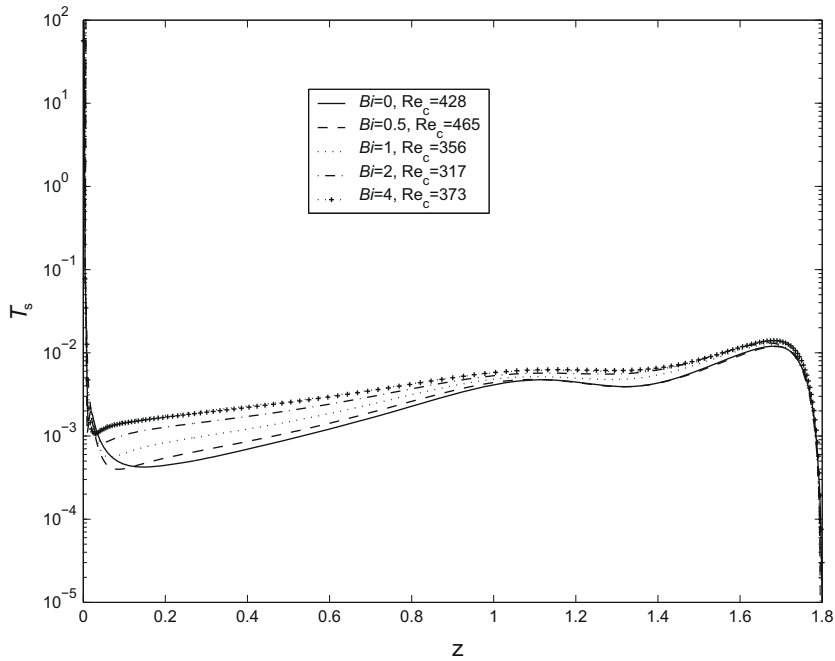
Fig. 7. Temperature gradient distribution on free surface at the corresponding Re_c for linear T_{amb} under normal gravity condition.
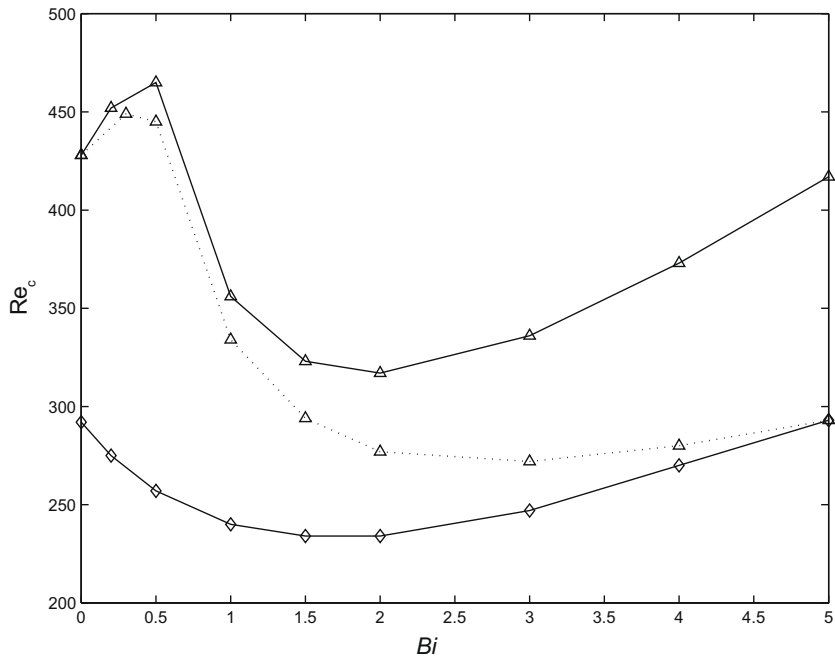

Fig. 8. Critical Reynolds number versus Bi for cases of linear ambient temperature ($g = g_0$, $Bo = 0$)-diamond points on solid line; ($g = g_0$, $Bo = 2.965$)-triangle points on solid line and ($g = g_0$, $Bo = 2.965$) when Biot number is set to zero in the perturbation equation (12)- triangle points on the dotted lines, respectively.

from the basic thermal field through the radial flow disturbances (J_1) always serves as the destabilizing effect. Both the thermal diffusion (D_{th}) and the effect involving the direct effect of interfacial heat transfer (Q) serve as the stabilizing effect, while the latter is much less important in the energy contribution. The energy transfer from the basic thermal field through the axial flow disturbances (J_2) also behaves as the stabilizing effect until it reverses to serve as the destabilizing effect at large Bi. The rate of change of "thermal" energy with the increasing interfacial heat transfer at $Re = 356$, the critical Reynolds number for the case ($Bi = 1$), is shown in Fig. 9b. It

can be seen that in the range of small Bi, the stability property of the stationary convection is determined by the contributions from the destabilizing energy transfer (J_1), the stabilizing energy transfer (J_2) and the thermal diffusion (D_{th}). The destabilizing energy transfer (J_1) overwhelms the heat diffusion (Q) and exhibits a local minimum around $Bi = 0.5$. On the other hand, the destabilizing energy transfer (J_2) nearly keeps constant until $Bi = 0.5$. The net effect of the coupling stabilizing energy transfer and the destabilizing energy transfer results in local maximum suppressing of the instability at $Bi = 0.5$ in the rate of the "thermal" energy (E_{th}) change of the
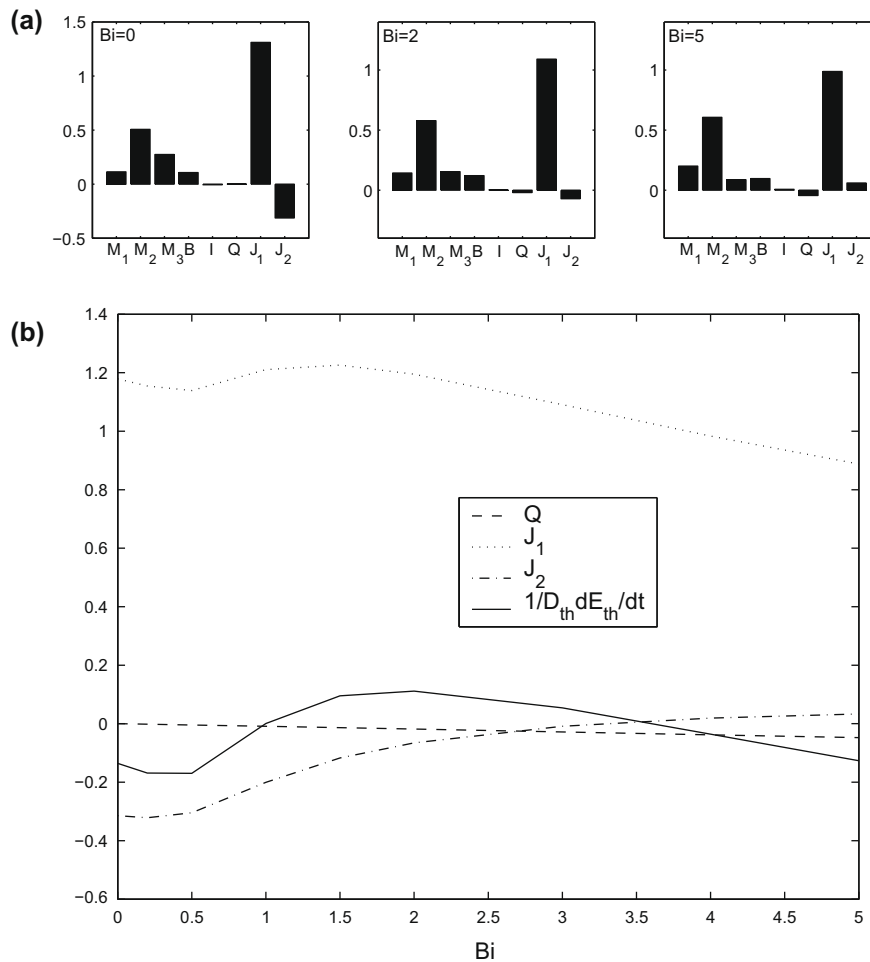
Fig. 9. Kinetic and thermal energy balance for cases of T_{amb} is linear when $g = g_0$, $Bo = 2.965$ (a) at the corresponding Re_c and (b) at Re = 356.

disturbance, which may relate to the appearance of the local maximum of the corresponding Re_c profile. Finally, the effect of melt free-surface deformation on the stability of the stationary convection was briefly studied as shown in Fig. 8. For the artificial case of under normal gravity condition but neglecting the melt free-surface deformation ($g = g_0$, $Bo = 0$), the corresponding Re_c profile exhibits a similar convex tendency as the case of under normal gravity. Noted that the profile does not exhibit any local maximum in the parameter range studied. The computed results also reveal the significant stabilization effect on the stationary convection through the modifications of the thermal and flow fields due to the free-surface deformation.

4. Conclusions

In the present paper, effect of interfacial heat transfer on the onset of oscillatory convection in liquid bridges formed by 1cst silicone oil on the ground is systematically studied in an extended range of Bi. With both the constant and linear ambient air temperature distributions, the numerical results show that the interfacial heat transfer modifies the free-surface temperature distribution directly and then induces a steeper temperature gradient on the middle part of the free surface, which may destabilize the convection. On the other hand, the interfacial heat transfer restrains the temperature disturbances on the free surface, which may stabilize the convection. The two coupling effects result in a complex dependence of the stability property on the Biot number, and the

appearance of the local maximum of the Re_c profile closely relates to the ambient temperature distribution. Moreover, the computed results reveal that the effect of free-surface deformation serves a significant stabilization on the two-dimensional axisymmetric stationary convection. To better understand the mechanism of the instabilities, rates of kinetic energy change and "thermal" energy change of the critical disturbances were also investigated. The "thermal" energy of the disturbances, which is important in liquid bridges of large Prandtl number, is mainly produced by the interaction between the basic thermal field and the flow disturbances and the thermal diffusion (D_{th}). The net work of the coupling effects above determines the stability property of the oscillatory convection.

Acknowledgment

References

[1] D. Schwabe, in: H.C. Freyhardt (Ed.), Crystals, vol. 11, Springer, Berlin, 1988, pp. 75–122.
[2] M. Levenstam, G. Amberg, C. Winkler, Instability of thermocapillary convection in a half-zone at in termediate Prandtl numbers, Phys. Fluids 13 (2001) 807–816.
[3] Y. Kamotani, L. Wang, S. Hatta, A. Wang, S. Yoda, Free surface heat loss effect on oscillatory thermocapillary flow in liquid bridges of high Prandtl number fluids, Int. J. Heat and Mass Transfer 46 (2003) 3211–3220.

[4] M. Irikura, Y. Arakawa, I. Ueno, H. Kawamura, Effect of ambient fluid flow upon onset of oscillatory thermocapillary convection in half-zone liquid bridge, Microgravity Sci. Technol. XVI-I (2005) 176–180.

[5] Y. Kousaka, H. Kawamura, Numerical study on the effect of heat loss upon the critical Marangoni number in a half-zone liquid bridge, Microgravity Sci. Technol. XVIII-3 (4) (2006) 141–145.

[6] A. Mialdum, V. Shevtsova, Microgravity Sci. Technol. XVI (2006) 146–149.

[7] D.E. Melnikov, V.M. Shevtsova, Thermocapillary convection in a liquid bridge subjected to interfacial cooling, Microgravity Sci. Technol. XVIII-3 (4) (2006) 128–131.

[8] A. Wang, Y. Kamotani, S. Yoda, Oscillatory thermocapillary flow in liquid bridges of high Prandtl number fluid with free surface heat gain, Int. J. Heat and Mass Transfer 50 (2007) 4195–4205.

[9] V. Shevtsova, Thermal convection in liquid bridges with curved free surfaces: Benchmark of numerical solutions, J. Crystal Growth 280 (2005) 632–651.

[10] G. Chen, A. Lizée, B. Roux, Bifurcation analysis of thermocapillary convection in cylindrical liquid bridges, J. Crystal Growth 180 (1997) 638–647.

[11] H.C. Kuhlmann, H.J. Rath, Hydrodynamic instabilities in cylindrical thermocapillary liquid bridges, J. Fluid Mech. 247 (1993) 247–274.

[12] G.P. Neitzel, K.T. Chang, D.F. Jankowski, H.D. Mittelmann, Linear stability theory of thermocapillary convection in a model of the float-zone crystal-growth process, Phys. Fluids A5 (1993) 108–114.

[13] G.H. Golub, C.F. Van Loan, Matrix Computations, Johns Hopkins University Press, Baltimore, 1996.

[14] C.H. Nienhüser, H.C. Kuhlmann, Stability of thermocapillary flows in non-cylindrical liquid bridges, J. Fluid Mech. 458 (2002) 35–73.

[15] D. Schwabe, Hydrothermal waves in a liquid bridge with aspect ratio near the Rayleigh limit under microgravity, Phys. Fluids 17 (2005) 112104.